Original Paper

Landslides
DOI 10.1007/s10346-023-02025-7
Received: 26 February 2022
Accepted: 19 January 2023

Daochuan Liu · Yang Jia · Yunyong He · Jiang Shao · Bo Xiang · Miao Liang · Fuming Wang · Chengchao Guo

Spatial–temporal characteristics of sediment transport by intermittent surges

Abstract Debris flows move as surge waves and they transport volumes of sediment of various magnitudes at irregular time intervals. As exemplified by Jiangjia Gully (JJG; Yunnan Province, China), the sediment transport of such surges can fluctuate by up to four orders of magnitude within a single debris flow event. This study investigated the variation of the sediment transported by a series of surges based on observations of 3000 surges in JJG. It was found that the fluctuation in sediment transport evolved with surge progress and then finally decayed in a power law form with a decay coefficient of 0.1–0.5, which can be considered a representative of the underlying dynamics. Moreover, the cumulative sediment yield followed a unified sediment size distribution (SSD) that can be expressed as $P(S) = CS^{-\beta}\exp(-S/S_c)$, with parameters well associated with the material composition of the surges. Moreover, this distribution also applies to transport processes in large-scale rivers, which suggests that the SSD could be used to predict the scale of sediment transport in rivers.

Keywords Sediment transport · Intermittent surges · Size frequency distribution · Flow fluctuation

Introduction

Debris flows are the major source of sediment in rivers (Slaymaker 1993; Lin et al. 2004; Tang et al. 2011), and the modulus of the sediment yield (M_s) can reach thousands to tens of thousands of tons per square kilometer per year (Cui 2000; Syvitski et al. 2007). This is much greater than that of large rivers, whose mean global annual sediment yield is just 190 t/km^2/a (Milliman and Farnsworth 2011). Even some mountain rivers with high sediment yield, e.g., certain rivers in the Transverse Ranges of southern California (USA) whose M_s is approximately 740–5300 t/km^2/a (Warrick and Mertes 2009; Warrick et al. 2015), do not transport as much sediment as that transported by debris flows.

There are three primary types of sediment transport process that operate in mountain gullies: steady fluvial transport from soil erosion, dramatic transport by floods, and debris flows. Compared with steady fluvial transport, sediment transport by floods from small watersheds is more transitory, the sediment concentration of which can increase to grams or hundreds of grams per liter in a short period (Conaway et al. 2013; Galewsky et al. 2006; Grodek et al. 2012), displaying marked spatiotemporal variability. However, steady fluvial transport always contains some sediment, and it shows minor fluctuation in the non-rainy season. In mountainous watersheds, debris flows and flood sediment transport might both occur during the same rainstorm event, but the behavior and sediment transport dynamics of debris flows are more complex than those of a torrential flood (Rickenmann et al. 2016; Rickenmann and Koschni 2010; Prancevic et al. 2014). In contrast to flood transport, high fluxes of sediment with a wide range of sizes and large boulders are always transported by debris flows, and the strong interactions of the solid and liquid constituents represent an essential element of debris flow mechanics (Iverson 1997; Li et al. 2015). The sediment transport of a debris flow is fundamentally different in terms of frequency and magnitude to that of a torrential flood (Hungr and Evans 2001; Wilford et al. 2004; Glade 2005; Liu et al. 2009). For example, the peak discharge of a debris flow is approximately 2–6 times greater than that of a torrential flood when they occur at the same frequency (Jiang 2015), highlighting the stronger sediment transport capability of debris flows.

Transport of solid material via intermittent surges is the typical mode of sediment transport in mountain watersheds globally (Davies 1986; Major 1997; Liu et al. 2009; Takahashi 2014; Li et al. 2015). Notable intermittent debris flow surges occur in Jiangjia Gully (JJG) of Yunnan Province (China) (Cui et al. 2005; Liu et al. 2009), and each debris flow event consists of tens or hundreds of surges with velocity in the range of 2–15 m/s, which can produce a yield of millions of cubic meters of sediment in just a few hours (Wu et al. 1990). According to investigation, the total amount of sediment transported by a debris flow could be tens or even hundreds of times greater than that of fluvial transport (Guo et al. 2013). The short-term sediment transport capacity of debris flows is far greater than that of large rivers.

Recent studies on debris flows based on numerical simulations and model tests have considered the influence of the nonuniformity of rainfall (Govindaraju et al. 2012; Lascelles et al. 2015), the Poisson process of soil instability (Li et al. 2011; Guo et al. 2014), and the silting or erosion of debris flow movement (Sepúlveda et al. 2015; de Lima et al. 2020). Additionally, a large amount of data obtained from field observation stations have been used to study the sediment transport capacity and hazards of mountain watersheds (Cui et al. 1999, 2005; Sadeghi et al. 2008; Warrick et al. 2015; Royall and Kennedy 2016; Imaizumi et al. 2016; Takayama et al. 2022). However, little attention has been given to the spatiotemporal characteristics of intermittent surges, the sediment they transport, or their dynamic processes. In this study, we examined the patterns of sediment transport by surges and investigated their fluctuation, probability distribution, and relationship with the material composition of debris flows. Finally, we also considered the sediment transport in large-scale rivers.

Study area and data collection

Study area

The area of focus of this study was JJG, which is located in the northeast of Yunnan Province (China). The river flows northward to join the Xiaojiang River, which is a major tributary of the upper Yangtze River. Overall, JJG covers an area of 48.7 km^2, and it extends for 13.9 km (Fig. 1). Slate and phyllite are intensely weathered in JJG, which results in a large number of shallow landslides, avalanches, and other loose deposits. Moreover, there is abundant rainfall in the JJG basin, i.e., the annual rainfall is in the range of 700–1200 mm. Given this background, debris flows in JJG appear in the form of surges with large-scale sediment transport under the excitation of concentrated rainfall. A site ideal for real-time observation of moving debris flows is the Dongchuan Observation and Research Station of Debris Flows (Dongchuan Station), operated by the Chinese Academy of Science.

Debris flow observation and data collection

Dongchuan Station has an automatic observation system, which has made continuous systematic observations and amassed a large dataset since its establishment in the early 1960s (Fig. 1). According to observation, approximately 15 debris flows occur in JJG annually. Each debris flow event consisting of tens or hundreds of surges typically persists for 3–4 h, but can continue for a period of tens of hours. The progress of a surge in the channel is shown in Fig. 2.

Kinetic parameters of debris flow surges such as depth (H), velocity (v), flow density (ρ), flow discharge (Q), and sediment yield (S) are measured using semiautomated instruments (Table 1). Flow velocity is measured by timing the surge front as it passes through two fixed cross sections. Fluid samples are collected from the moving surges using a suspended cable sampler measuring 0.3 m^3, and the density is obtained directly by weighing the fluid. The maximum discharge is 2820 m^3/s (equivalent to 5 times the peak discharge of the Xiaojiang River), the maximum velocity is 15 m/s, the maximum depth is 5.5 m, the flow density is 2.37 g/cm^3, the maximum sediment transport rate is 6079 t/s, and the maximum amount of solid runoff is approximately 2×10^6 m^3.

Methods

From a macro perspective, a debris flow is equivalent to a surge series that is expected to feature the following intrinsic property:

$$X = \{ X_i | i = 1, 2, 3, \cdots, N \} \tag{1}$$

where X is the parameter observed in real time (e.g., H, v, ρ, Q, and S) and N is the surge number of the debris flow event.

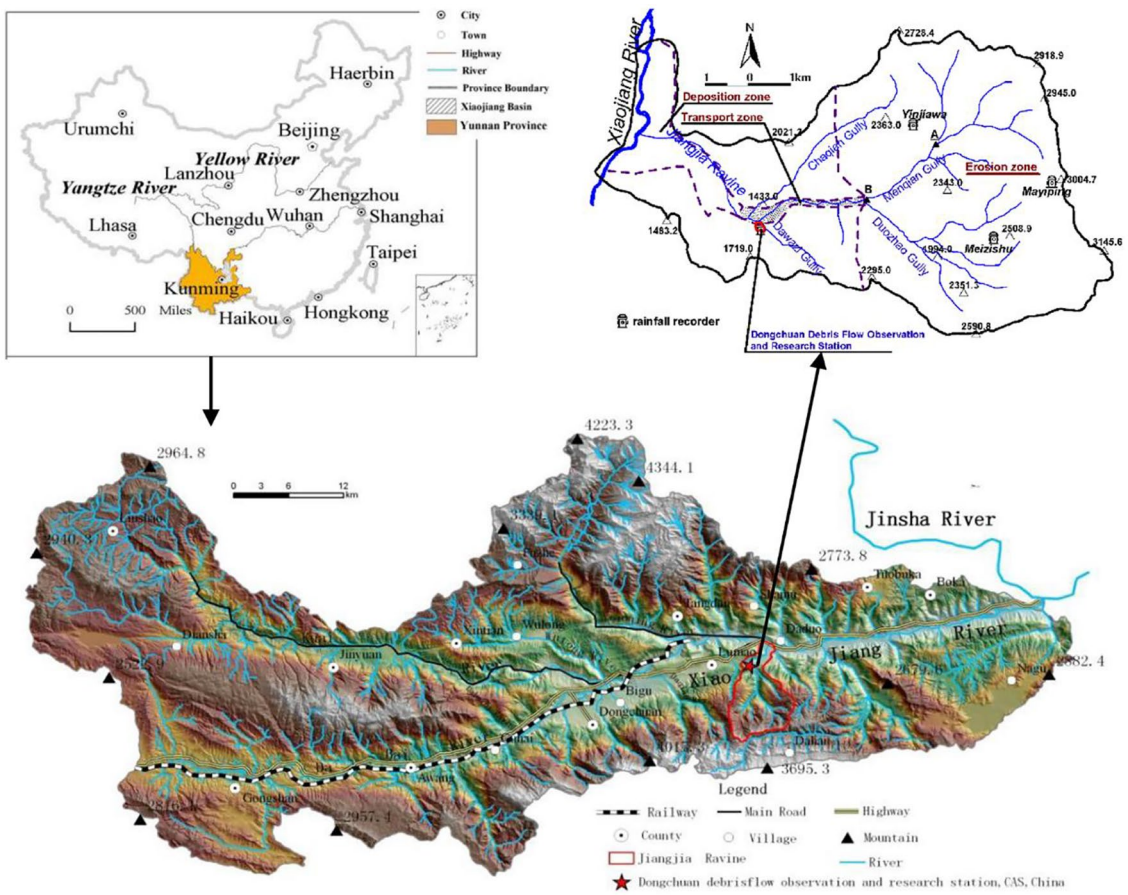

Fig.1 Location of the Xiaojiang basin and Dongchuan observation station

(a) Intermittent surges of debris flow **(b)** Movement progress of surges

Fig. 2 Intermittent surge of a debris flow in the JJG

Field investigation has revealed that obvious fluctuation and variety exist in the process of sediment transport by intermittent surges. Therefore, the standard deviation (σ) and variation coefficient (*CV*) are used to describe the temporal variation of sediment transport. Thus, the physical meaning of σ is to describe the fluctuation of the series, which varies temporally in a debris flow series and can be defined as follows:

$$\sigma_n = \sqrt{\frac{\sum_{i=1}^{n} (X_i - \langle X \rangle_i)}{i}} \tag{2}$$

where the range of n is $[1, N]$ and $\langle X \rangle$ is the mean value.

Here, *CV* is used to discuss the relative standard deviation and variability. Generally, the larger the value of *CV*, the stronger the variability; the formula can be expressed as follows:

$$CV = \frac{\sigma}{\langle X \rangle} \times 100\% \tag{3}$$

Most debris flow series in nature exhibit long-range correlation and self-similarity characteristics, which can be considered representative of the underlying dynamics. Therefore, a cumulative distribution model is often used to describe the magnitude–frequency relationships of such series (Eagleson 1972; Yue et al. 1999; Aronica and Candela 2007; Read and Vogel 2016), and the parameter distributions can generally be fitted by the Weibull distribution or even a more general distributional function involving power and exponential components (Li et al. 2005 2007). Observational data from JJG reveal that the sediment yield of the intermittent surges fluctuates intensely. To explore the kinetic effect of sediment transport by intermittent surges, the cumulative distribution is used to express the

Table 1 Flow parameters of debris flow event 010,813 in the JJG

Surge number	Duration T (s)	Velocity v (m/s)	Discharge Q (m³/s)	Density ρ(g/cm³)	Runoff Q_c (m³)	Sediment yield S (m³)
1	26	7.77	285.90	2.20	3145.00	2286.00
24	23	8.67	499.40	2.30	4744.00	3738.00
25	23	8.85	575.20	2.30	4889.00	3852.00
26	34	5.88	185.20	2.30	3148.00	2481.00
27	21	9.39	563.40	2.30	4226.00	3330.00
39	27	7.44	285.70	2.15	2857.00	1992.00
53	26	7.72	463.20	2.25	2779.00	2106.00
54	30	6.63	298.40	2.25	6266.00	4750.00
83	30	6.74	242.60	2.27	3882.00	2989.00
117	37	5.37	193.30	2.10	5606.00	3739.00
118	30	6.68	300.60	2.20	3758.00	2732.00
122	21	9.62	793.60	2.25	15,078.00	11,430.00
123	22	9.00	742.50	2.25	11,509.00	8724.00
124	29	6.93	360.40	2.25	4144.00	3142.00
193	70	2.86	254.20	1.70	2040.00	865.00

magnitude–frequency relationships and the integrality of surges in debris flow events.

Results

Temporal variation of sediment transport

Fluctuation and decay of sediment yield

Hydrographs of debris flow events 910709, 010813, and 910813 indicating discharge and sediment yield are shown in Fig. 3. Three fundamental parameters, density (ρ, g/cm^3), velocity (v, m/s), and duration (T, s), are used to determine the discharge and sediment transport process, which is shown in a ternary array (ρ, v, T). The sediment transport exhibits various patterns: a single peak, multiple peaks, and their irregular combination. Debris flow event 040721 has a typical single-peak hydrograph of sediment transport (Fig. 4a-1). The majority of surges in such hydrographs have little sediment yield, with just one or two isolated peaks transporting large volumes of sediment, thereby showing strong variability in the process of sediment transport. However, some sediment transport hydrographs are often characterized by multiple peaks (e.g., events 910711, 010813, and 910813; 910813 is shown in (Fig. 4b-1), whose σ and CV values are smaller than those of single peaks (Table 2), which means that their fluctuation and variation are smaller than those of the single-peak patterns. Additionally, the combination types contain some single peaks and clusters of multiple peaks (Fig. 4c-1), reflecting wide-ranging variation.

During the advance and evolution of surges, dramatic variation in sediment yield indicates that huge fluctuations exist in the sediment transport process. Notably, the decay of a fluctuation in the process of sediment transport generally occurs after a flood peak. However, the smooth decay process can suddenly jump and then recommence the decay process when a subsequent larger peak is encountered (Fig. 4c-2). This indicates that the local maximum sediment yield is the key factor in determining the sediment transport process. Despite the abrupt variation in the early part of an entire series, σ_n finally varies with surge number in a power-law form:

$$\sigma_n \sim n^{-\alpha} \tag{4}$$

Notably, the range of exponent α is approximately 0.1–0.5 for all the debris flow events (Table 2). The decay coefficient α of most events of multiple-peak type is smaller than that of the other two types (Table 2), suggesting that the local relative fluctuation of multiple peaks is slightly less than that of the other types. The decay properties of a surge series show that the movement process of a debris flow is not stochastic, but that it has certain nonlinear dynamic characteristics.

Additionally, to show the overall fluctuation of the sediment yield series, the σ values of all the debris flow series are listed in Table 2. Except for a few events, the value of σ is in the range of 0.9–10 × 10^3 m^3, showing little difference between the three patterns. Therefore, we introduce the CV to discuss the relative standard deviation and variability. It is worth noting that the CV values of the three sediment transport patterns are markedly different (Table 2). The highest CV values, i.e., in the range of 170–540%, are associated with the single-peak pattern and are much higher than the values for the multi-peak (CV: 70–120%) and combination (CV: 120–170%) types.

Fluctuation of surges with different density

The diverse ranges of depth, velocity, and sediment transport under the same flow density lead to fluctuation in intermittent surges. We chose all sediment yields at a given density as a new series, where similar fluctuations are also presented. For example, at density of 2.0 g/cm^3 (considering the accuracy of density measurements, statistical analysis was performed on flows with density of between 1.95 and 2.05 g/cm^3); the sediment yield is in the range of 1.8 m^3 to 40.649 × 10^3 m^3, with an average value of 3.06 × 10^3 m^3; and the values of σ and CV at different densities are 0.4–8 × 10^3 m^3 and 100–280%, respectively. Most importantly, the value of σ increases broadly with flow density in the form of an exponential relationship, for which the R^2 value of 0.817 indicates the goodness of fit (Fig. 5). This means that high-density surges usually have more abundant sediment transport and relatively high fluctuation. Actually, high-density surges have a complex and variable grain composition; thus, their fluctuation can be attributed to grain composition, as discussed in "Discussion and application".

Upper limit of sediment transport series

The S_{max} of a surge series determines the range of fluctuation. Therefore, we consider the effect of S_{max} on the sediment transport series, which might vary with surge properties, e.g., flow density and velocity. Consideration of the variation of S_{max} with flow density and velocity reveals that S_{max} increases with density as a power law function:

$$S_{max} = k\rho^p \tag{5}$$

The statistics yield values of $k = 0.0315$ and $p = 10.16$ ($R^2 = 0.9868$) (Fig. 6a). A similar limit also exists between velocity and S_{max} (Fig. 6b):

$$S_{max} \sim v^r \tag{6}$$

for which the statistics yield a value of $r = 1.60$ ($R^2 = 0.99$). Equations (5) and (6) also suggest that the high density and velocity of surges usually have a relatively high limit and high fluctuation of sediment yield.

Sediment size distribution (SSD) of sediment transport

The previous analysis suggests that there should be a dynamic process to describe the decay properties, fluctuation, and variability of a surge series. Although the underlying dynamics are unknown, there are tangible properties that reflect the integrity of a surge series. It has been found that sediment yield, despite its marked fluctuation, shares a cumulative distribution described by the following statistical result:

$$P(S) = CS^{-\beta} \exp(-S/S_c) \tag{7}$$

where $P(S)$ is the percentage of surges with sediment yield of $> S$, C is a coefficient, β is a power exponent, and S_c is the characteristic sediment yield as defined above. All three parameters can be determined by fitting Eq. (7) to the sediment yield data of a surge series. The unified cumulative distribution (Eq. (7)) shows that a surge series behaves as an entity that obeys a unified dynamical framework that encompasses all appearances.

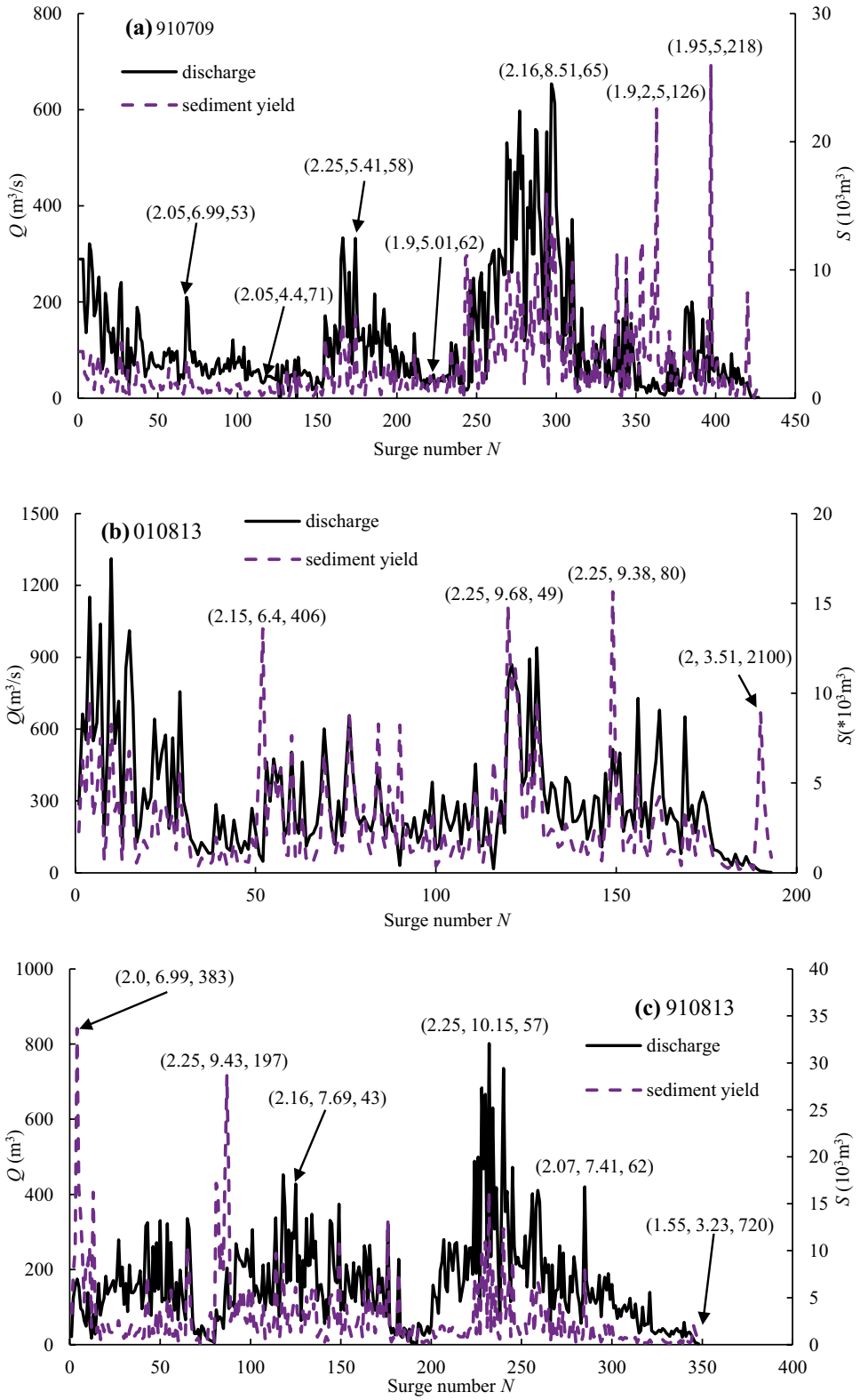

Fig. 3 Hydrographs of debris flow events 910709, 010813 and 910813

Moreover, when we rescale the sediment fluctuation by S_c and normalize the percentage as $P(S)S^{\beta}/C$, Eq. (7) can be rewritten as $P^*(S) = \exp(-S/S_c)$, leading to the curves collapsing onto a single scaling curve of exponential $\exp(-S/S_c)$ (Fig. 7). The meaning of each individual SSD parameters is discussed in the following section.

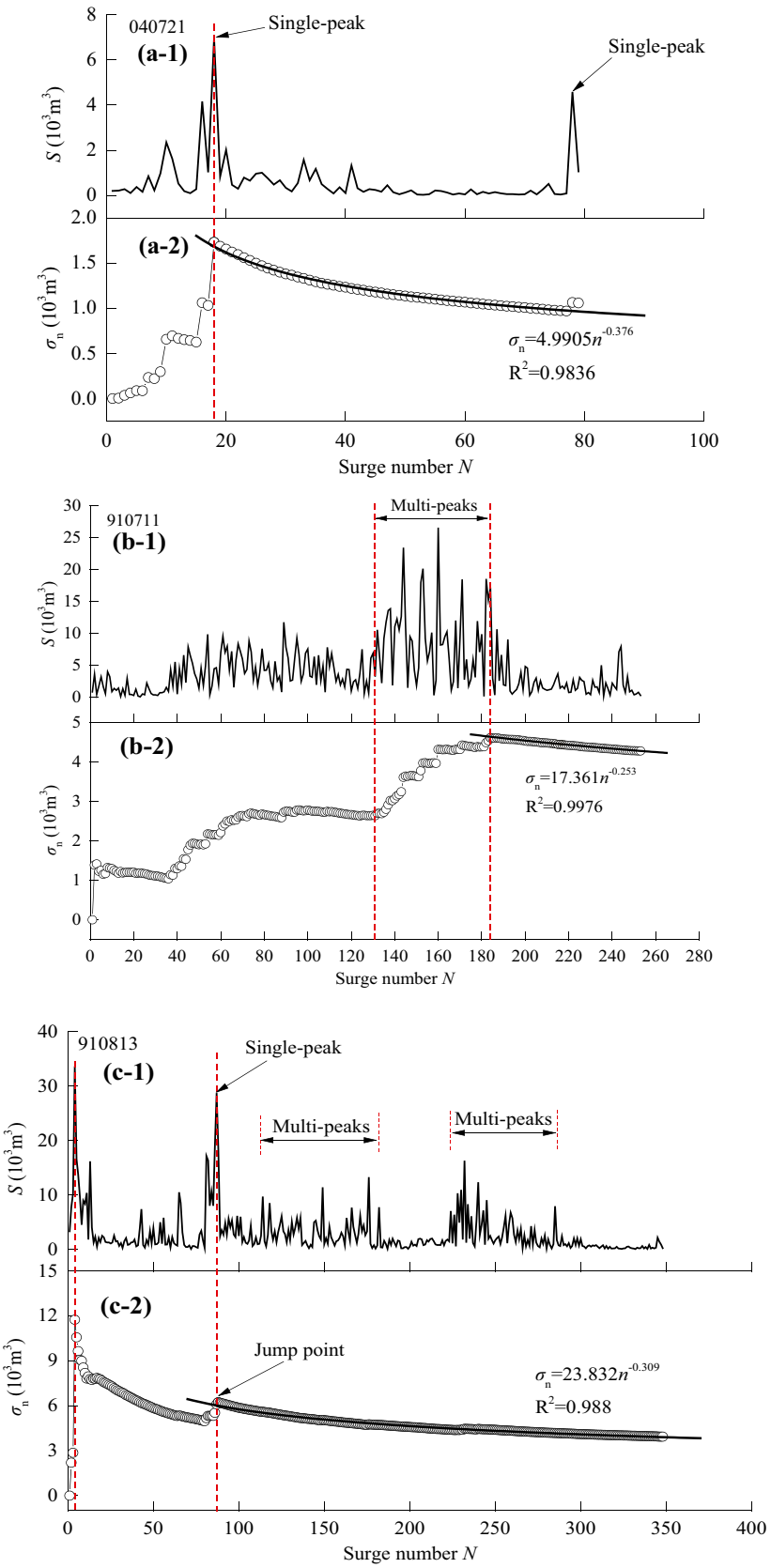

Fig. 4 Standard deviation variation (σ) with progression of surge series

Table 2 Statistical parameters of sediment discharge in surge series

Sediment yield pattern	Event	α	$\langle S \rangle$ ($10^3 m^3$)	σ ($10^3 m^3$)	S_{max} ($10^3 m^3$)	CV (%)
Multiple peaks	890802	0.114	0.8562	0.6721	3.3736	78.49
	890803	0.153	0.4658	0.4283	2.8145	91.96
	910711	0.255	4.2805	4.2888	26.5540	100.20
	970725	0.348	2.6729	3.1293	28.6910	117.08
	970829	0.322	2.9432	2.6060	16.5940	88.54
	990716	0.223	4.7514	5.2588	39.2700	110.68
	990810	0.278	1.7844	1.7190	9.6140	96.34
	990818	0.232	1.7214	1.4805	7.6370	86.01
	990825	0.307	2.7545	3.0816	20.2000	111.85
	990829	0.258	2.3018	2.3412	18.4720	101.71
	010813	0.294	2.7676	2.7061	15.6420	97.78
	010822	0.288	4.5197	4.6230	24.4940	102.29
	020820	0.365	3.0951	3.2502	21.0220	105.01
	030611	0.262	3.6242	3.1475	18.9170	86.85
	030726	0.096	1.6143	1.4063	5.4120	87.12
Irregular combinations	890627	0.312	2.7527	3.7384	20.5107	135.81
	910709	0.271	2.3324	2.9394	26.0229	126.02
	910813	0.309	2.8353	3.9375	33.6617	138.87
	940616	0.386	5.3003	8.9701	80.7878	169.24
	990724	0.218	1.8701	2.3386	12.7840	125.05
	020718	0.239	1.4724	1.8911	9.3440	128.43
	020816	0.218	3.4338	5.5452	45.4120	161.49
Single peak	970707	0.329	2.0989	5.6405	76.3560	268.73
	970715	0.452	10.455	40.9159	425.8870	391.36
	010708	0.376	1.4606	2.5955	23.9060	177.70
	040721	0.476	0.6035	1.0651	6.9620	176.48
	040825	0.376	6.9604	34.756	244.6850	499.34
	070726	0.428	1.7592	2.6270	13.4220	149.32
	020815	0.330	7.3224	18.3723	107.3950	250.91

SSD parameters of C, β, and S_c

Independent variables The three SSD parameters C, β, and S_c are calculated directly from data fitting of Eq. (7) and are listed in Table 3. Surprisingly, the β–C relationship appears in the form of a logarithmic function with reasonable goodness of fit (Fig. 8):

$$\beta = a\ln(C) + b \tag{8}$$

where $a = -0.389$ and $b = 1.7968$, with $R^2 = 0.96$. The exact correlation between β and C indicates that they are not independent variables. Statistical analysis reveals that β in JJG has a logistic distribution (Fig. 9), with an average and standard variance of − 0.038 and 0.006, respectively. In summary, the sediment size distribution holds for all sediment yields of a series of debris flow events and the distinction depends only on parameters β and S_c.

Size effects on SSD parameters We found that the range of β is from − 0.23 to 0.2 and that of S_c is 0.5–110. As shown in Fig. 10, the variations of β and S_c show diverse patterns in the sediment transport series. It is noted that the values of β and S_c of the single-peak

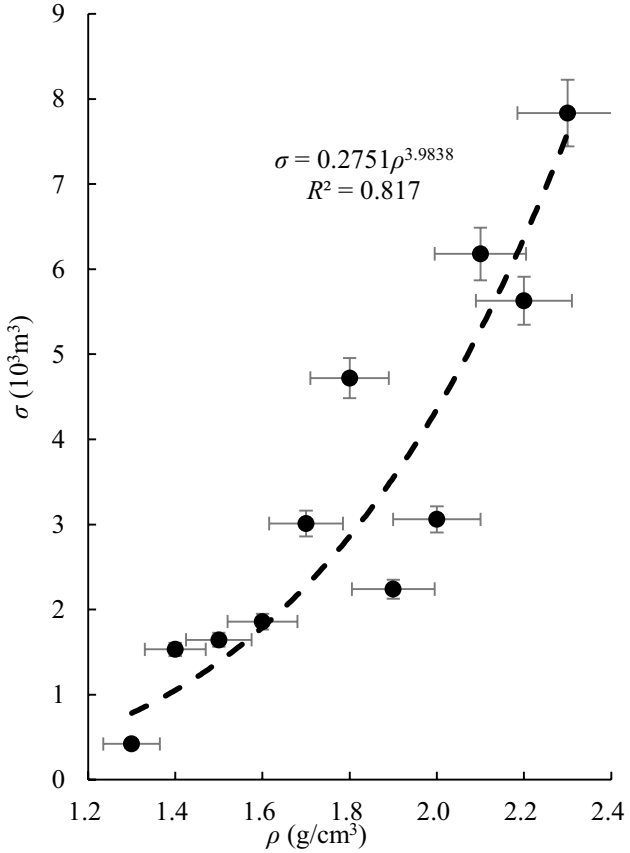

Fig. 5 σ varies with the flow density ρ in JJG (5% error line)

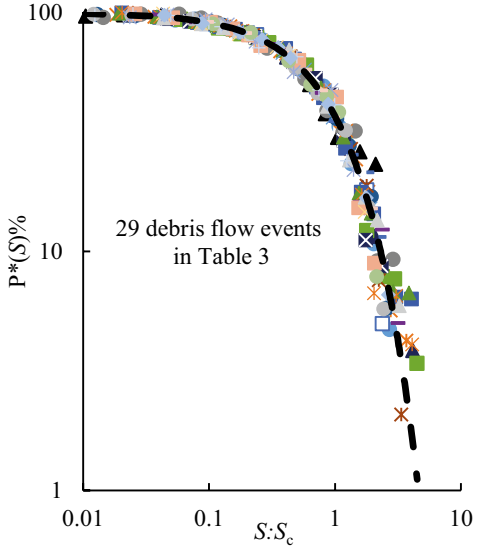

Fig. 7 Exponential distribution of sediment yield of debris surges

patterns are 0–0.2 and 4–110, respectively, which differ markedly from those of the multiple-peak and combination patterns, i.e., $\beta < 0$ and $S_c = 0.5–13$ (Table 4). The SSD parameters of the three patterns are listed in Table 4.

For the multiple-peak sediment yield series, parameters β and S_c exhibit a degree of an exponential relationship with $R^2 = 0.9121$ (Fig. 11a). For the combination type, a weak exponential relationship still exists for the parameters β and S_c (Fig. 11b). However, if there is a sudden increase in the amount of sediment yield for one or two surges, the similarity of the relationship between β and S_c with the single-peak pattern disappears (Fig. 11c). The β–S_c relationship shown in Fig. 11a implies that underlying system dynamics might operate because of the self-similar structure of the channel network and the self-organized nature of soil failure criticality. Nevertheless, a single-peak point in the series will break the self-organized rules and yield different features of sediment transport.

Fig. 6 Fluctuation of sediment yield for debris flows in the JJG (5% error line)

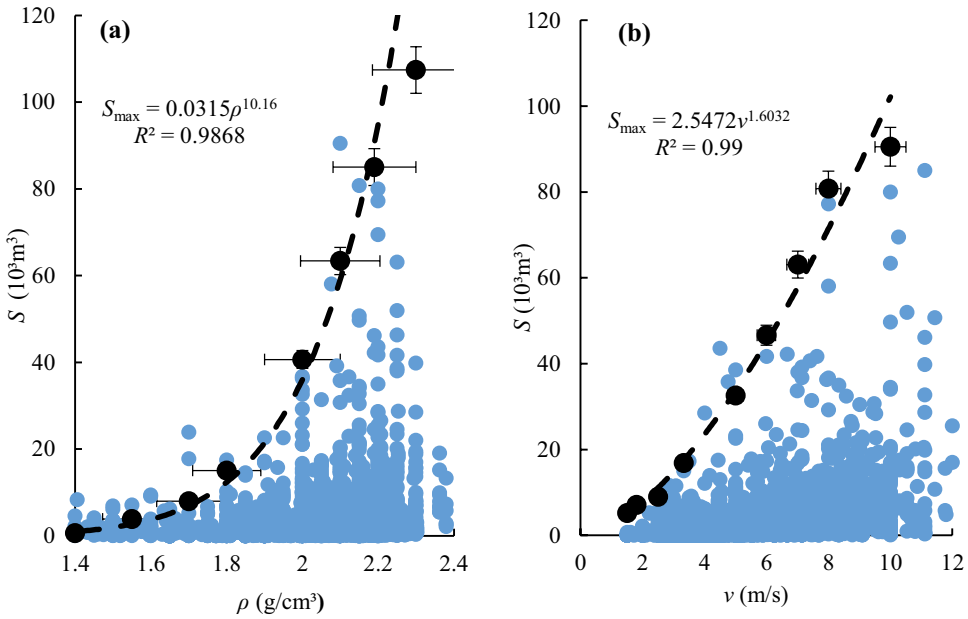

Table 3 Parameters of sediment discharge in a surge series

Sediment yield pattern	Event	C	β	S_c ($10^3 m^3$)	R^2
Multiple peaks	890802	179.1857	− 0.2212	1.0090	0.9992
	890803	212.4052	− 0.2442	0.4825	0.9971
	910711	113.4966	− 0.0641	7.3865	0.9928
	970725	114.5095	− 0.0576	4.8818	0.9932
	970829	125.8221	− 0.1072	3.7707	0.9881
	990716	111.4397	− 0.0536	8.5370	0.9883
	990810	128.8974	− 0.1013	2.5209	0.9959
	990818	132.8764	− 0.1115	2.2533	0.9985
	990825	113.3607	− 0.0510	5.1525	0.9947
	990829	124.7006	− 0.0961	3.3541	0.9918
	010813	117.4406	− 0.0676	4.4649	0.9978
	010822	110.6117	− 0.0478	8.3786	0.9962
	020820	115.8544	− 0.0621	4.9275	0.9945
	030611	120.1986	− 0.0810	4.6045	0.9936
	030726	134.9314	− 0.1266	2.3154	0.9916
Irregular combinations	890627	104.4533	− 0.0115	8.2093	0.9959
	910709	107.9923	− 0.0226	5.4145	0.9986
	910813	105.0444	− 0.0128	7.7289	0.9986
	940616	104.2300	− 0.0139	13.9848	0.9900
	990724	110.5012	− 0.0338	4.4399	0.9948
	020718	109.3796	− 0.0342	3.8760	0.9867
	020816	108.8338	− 0.0260	6.8252	0.9797
Single peak	970707	97.2154	0.0273	9.5015	0.9841
	970715	96.6926	0.0254	181.5249	0.9735
	010708	92.2389	0.0558	6.9155	0.9902
	040721	80.5009	0.1046	4.2538	0.9897
	040825	95.2292	0.0369	90.6748	0.9854
	070726	96.1753	0.0296	8.0217	0.9827
	020815	96.0838	0.0395	46.1163	0.9766

Physical meaning of SSD parameters

As shown in Fig. 7, the curves fall abruptly at point $S/S_c = 1$; thus, S_c can be treated as a critical point and defined as the characteristic sediment yield. Then, the meaning of parameter S_c can be explained by the variation of S_c with the S_{max} and σ of the sediment transport series. It can be seen from Figs. 12 and 13 that S_c increases positively with S_{max} and σ for all three sediment transport patterns. Such statistical results clearly illustrate the physical meaning of parameter S_c, which can broadly characterize the degree of fluctuation and the maximum sediment transport capacity of a debris flow series.

It is evident that there are more surges with sediment yield below S_c ($S_{S<Sc}$) in the debris flow event. For single-peak patterns in particular, if we assume that there are τ sediment yields that are less than parameter S_c ($S_{S<Sc}$) in a debris flow event, the percentage of τ can be written as $N(S<S_c) = \tau/N^*100$, where $N(S<S_c)$ accounts for 95–98% of the total, i.e., much larger than that of the multiple-peak and combination types. It is also worth noting that irrespective of the type of pattern, the sediment contribution by surges with $S_{S<Sc}$ accounts for 55–80% of the total sediment yield. This indicates that surges with $S_{S<Sc}$ are the main contributors of sediment transport in debris flow events.

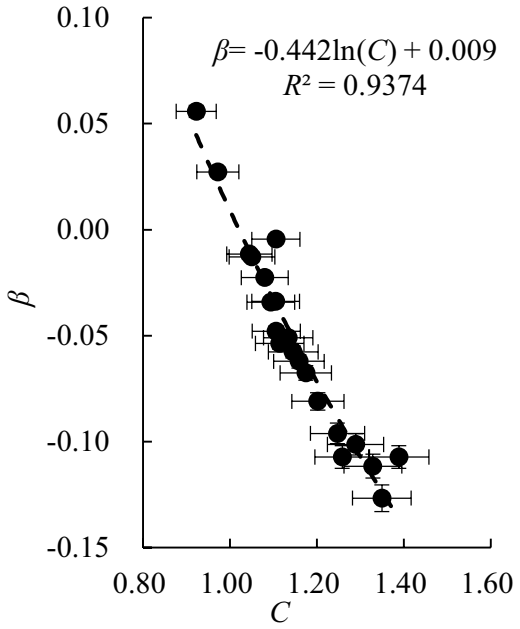

Fig. 8 β-*C* relationship of the distribution (5% error line)

Additionally, parameter β increases with $N(S<S_c)$ (Fig. 14), suggesting that exponent β is related to surges in a series with sediment yield of below S_c ($S_{S<Sc}$). Taking S_c as the representative magnitude of a series, results show that the largest percentage of "small" surges (e.g., surges with $S_{S<Sc}$) usually presents a high decay exponent α (Table 4). Specifically, comparison of the three different pattern series of 040721, 910711, and 910813 (Fig. 4) reveals that they have the same decay characteristics at the end of the surge series; however, 040721, with higher values of β and $N(S<S_c)$ falls more steeply (Fig. 4).

The variation of SSD parameters reflects the different sediment transport patterns and the magnitude of fluctuation in debris flow events. In practice, β is positive for a single-peak pattern and negative for the other two pattern types. Furthermore, the greater the percentage of "small" surges, the bigger the value of exponent β and the higher the decay rate. Conversely, S_c defines the characteristic sediment yield that governs the fluctuation and capacity of sediment transport. This means that β and S_c take the role of an integrated index that can describe the fluctuation of sediment transport in a debris flow series. The uniform size frequency distribution of sediment yield reflects the integrity and systematic nature of debris flows. This integrity can result in a wide range of debris flow surge evolution patterns in similar mountain watersheds, which results in fluctuation of the sediment yield within debris flows.

Discussion and application

Effects of granular composition on sediment transport

Observations indicate that successive surges usually have different densities and consist of different materials, meaning that they are more likely to have emerged from different tributaries and sources. More importantly, material composition plays an important role in the activity of a debris flow (Li et al. 2005, 2007). Therefore, the constraints on sediment transport fluctuations imposed by flow density and velocity (Fig. 6) can be attributed to grain composition.

The material comprising a debris flow satisfies the universal grain size distribution of $P(D)=CD^{-\mu}\exp(-D/D_c)$, and the grain composition is determined by the grain parameters μ and D_c (Li et al. 2013; 2017). Broadly, the value of μ represents the porosity of a debris flow, where a small value of μ implies low porosity and possibly high excess pore pressure in the debris flow, reflecting high mobility and high transport capacity. A large value of D_c means a wide range of grain composition in the debris flow (Li et al. 2013, 2017). Moreover, flow

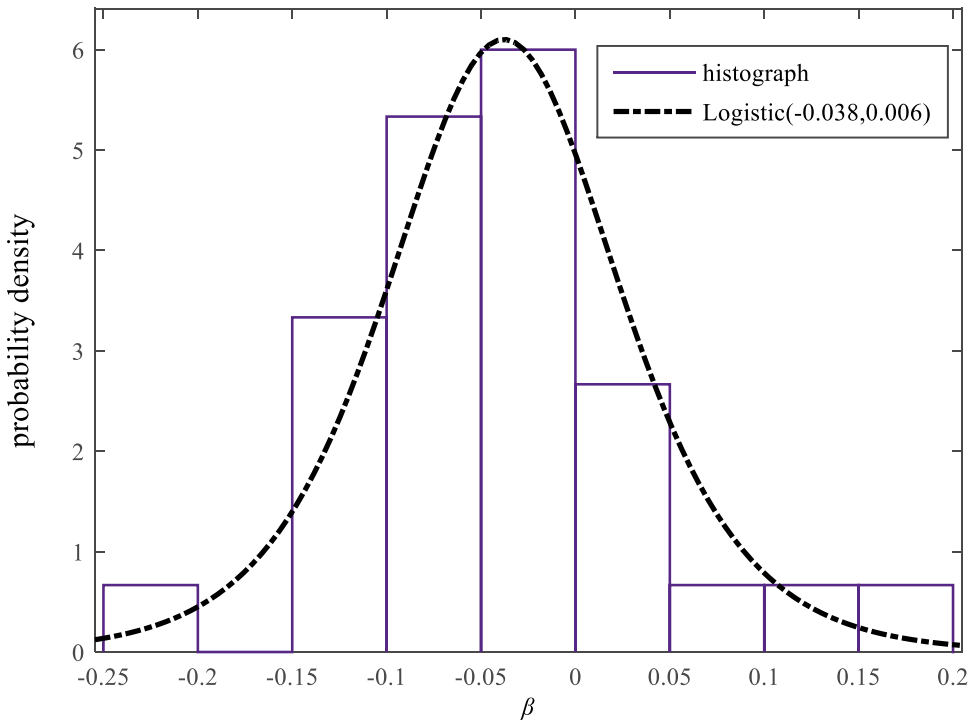

Fig. 9 Probability density of parameter β in the JJG

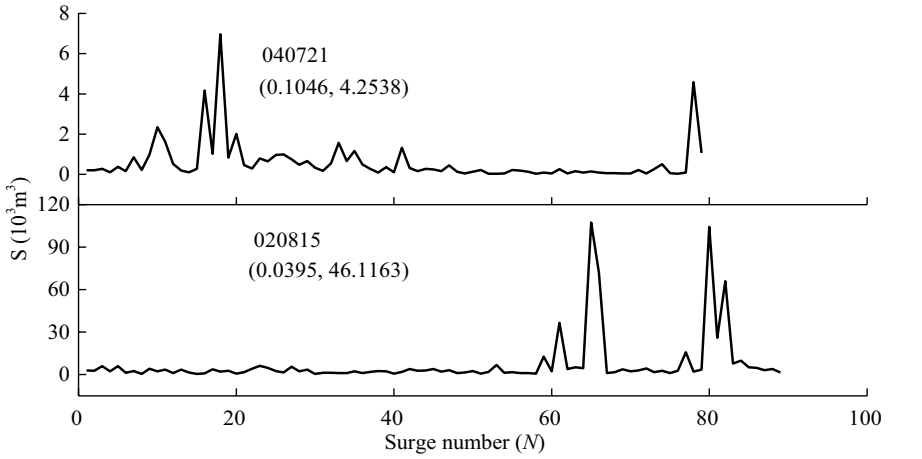

(a) Single peak hydrographs

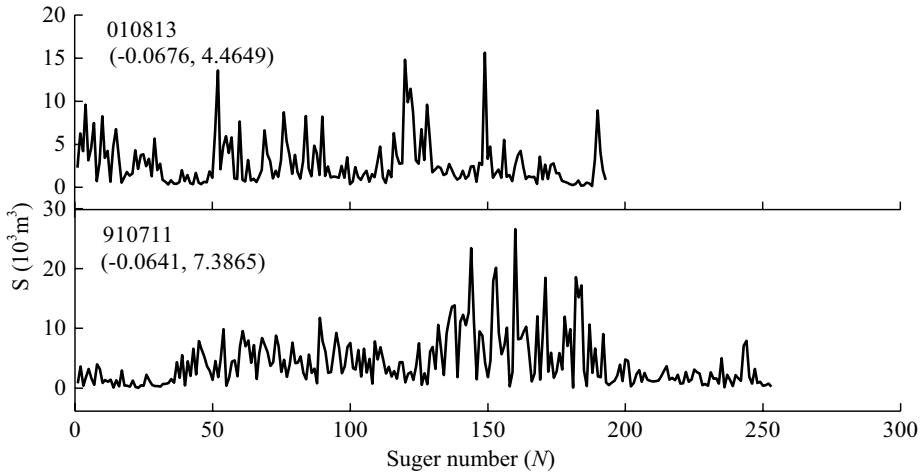

(b) Multiple peaks hydrographs

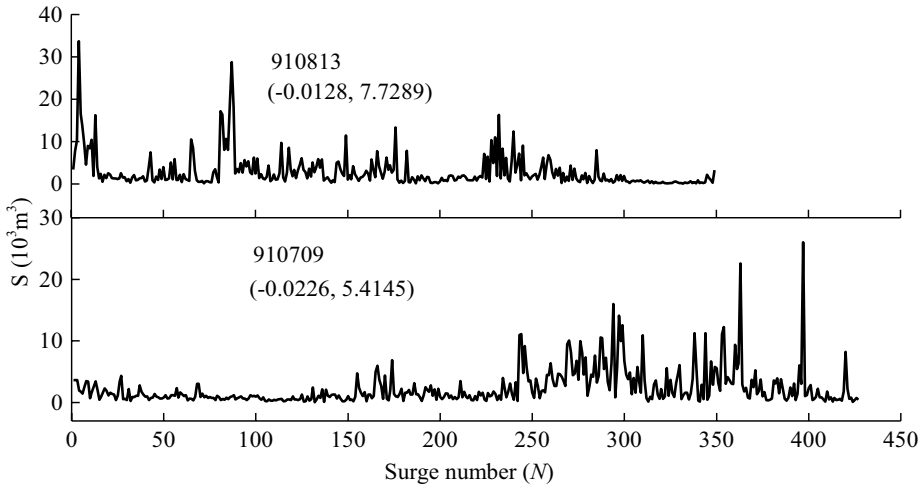

(c) Irregular combinations

Fig. 10 Sediment yield of some debris flow events. Values in parentheses represent the SSD parameters (β, S_c); the various of the (β, S_c) shows diverse patterns of sediment transport series

Table 4 Sediment transport patterns classification by SSD parameters

Patterns	SSD parameters			α	*CV* (%)	σ (10^3m^3)
	C	β	S_c (10^3m^3)			
Milt-peaks	110 ~ 140	− 0.23 ~ − 0.04	0.5 ~ 8.5	0.09 ~ 0.35	70 ~ 120	0.4 ~ 5
Combinations	100 ~ 110	− 0.04 ~ 0	3 ~ 13	0.21 ~ 0.39	120 ~ 170	1.8 ~ 9
Single peak	65 ~ 100	0 ~ 0.2	4 ~ 110	0.33 ~ 0.48	170 ~ 540	2.5 ~ 34

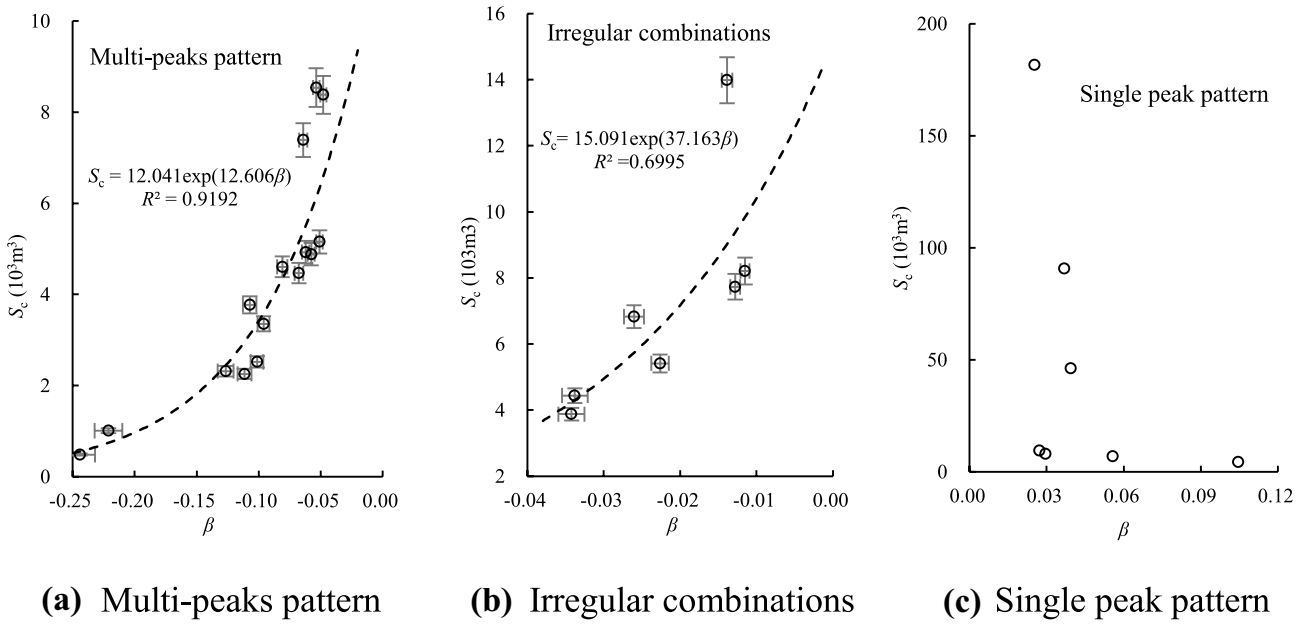

(a) Multi-peaks pattern **(b)** Irregular combinations **(c)** Single peak pattern

Fig. 11 β-S_c relationships of different sediment yield series patterns

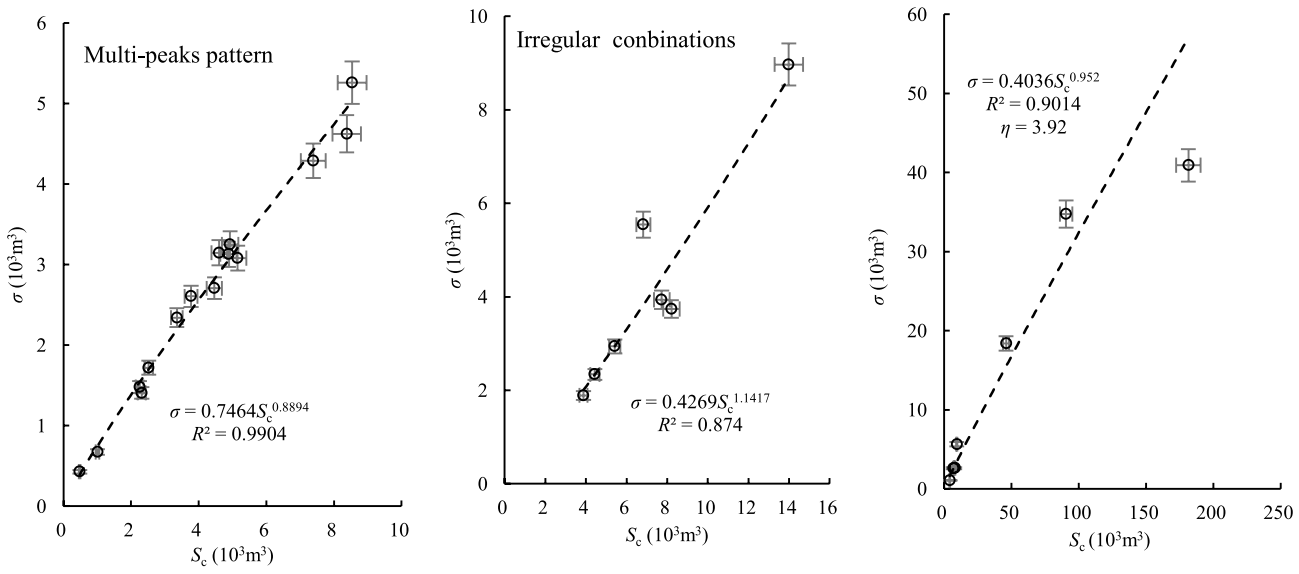

(a) Multi-peaks pattern **(b)** Irregular combinations **(c)** Single peak pattern

Fig. 12 σ-S_c relationships of different sediment yield series patterns

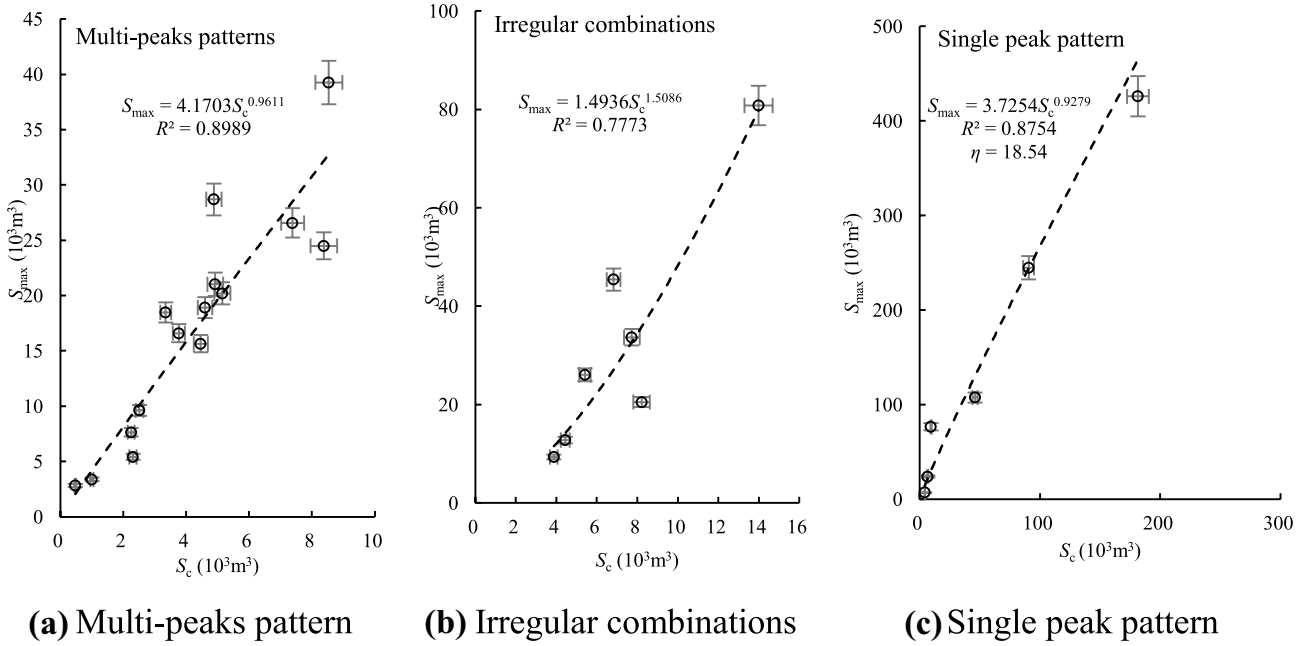

Fig. 13 S_{max}-S_c relationships of different sediment yield series patterns (5% error line)

density ρ can be described by the parameters μ and D_c (Li et al. 2013), and the power exponential relationship can be expressed as follows:

$$\rho \sim \mu^{-a}, \rho \sim D_c^{\,b} \tag{9}$$

Considering the relationship between flow density ρ and σ (Fig. 5), an approximate relationship between σ and the parameters μ and D_c can be expressed as follows:

$$\sigma \sim \mu^{-M}, \sigma \sim D_c^{\,N} \tag{10}$$

This suggests that grain composition plays an important role in the fluctuation of debris flow surges. Generally, the clay content in high-density debris flow surges with $\mu < 0.05$, and $D_c \sim 20$ mm is much greater than that of low-density debris flow surges with $0.05 < \mu < 0.1$ and $2 < D_c < 15$ mm (Li et al. 2013), which creates a

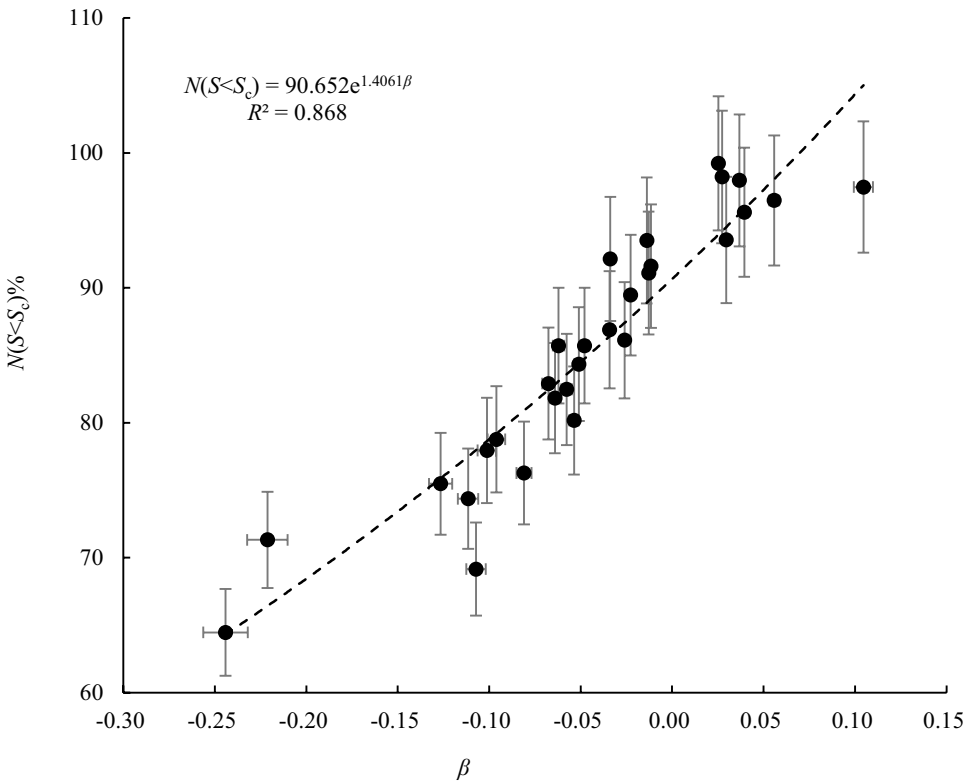

Fig. 14 β-$N(S < S_c)$ relationship for debris flows in the JJG (5% error line)

Table 5 Parameters of interannual sediment yield series of different basin (from 1955 to 1990)

River	Hydrologic station	*CV* (%)	SSD parameters			R^2
			C	β	S_c ($10^7 m^3$)	
Wuding River	Baijiachuan	85.08	112.56	− 0.0540	8.39	0.9844
Beiluohe River	Liujiahe	64.05	129.89	− 0.0994	2.81	0.9911
Beiluohe River	Jiakouhe	57.58	115.29	− 0.0957	13.57	0.9862
Weihe River	Huaxian	63.44	135.15	− 0.1228	2.90	0.9937
Weihe River	Xianyang	67.27	134.60	− 0.1207	2.85	0.9964
Jinghe River	Zhangjiashan	59.40	117.01	− 0.0881	10.43	0.9902
Yellow River	Huayuankou	39.32	151.80	− 0.1972	28.01	0.9017
JJG	JJG	131.48	101.70	− 0.0056	0.044	0.9814

strong internal structure, high yield stress, and high excess pore pressure. It also leads to a larger content of coarse grains that participate in the structure of the debris flow (Li et al. 2013) and show strong carrying capacity of sediment. Data from JJG also show that the sediment concentration of surges has a positive relationship with parameter D_c (Li et al. 2015). However, a process of paving the gully bed occurs when high-density debris flow surges move, which reduces the Manning coefficient of the gully bed by approximately half (Du et al. 1987). Consequently, subsequent surges can maintain a state of high-velocity motion. With increase in flow velocity, the turbulent motion of the fluid is enhanced, which increases the quantity of coarse grains in suspension and increases the sediment transport capacity of the debris flow. However, debris floods (density: 1.3–1.6 g/cm^3) in a series have severe erosive effect on the gully bed and roughen the active path in the process of movement, thereby reducing the velocity of the debris flood surges and lowering the sediment transport capacity and degree of fluctuation. Thus, these two mechanisms explain the results shown in Figs. 5 and 6.

Application of SSD in sediment transport in the Yellow River Basin

Sediment transport by a river is more persistent and stable than that by a debris flow, but river sediment still shows interannual fluctuation. Irrespective of whether by debris flow in a small-scale gully or by a large-scale river, sediment transport is the result of a discontinuous and random supply of sediment material. Therefore, it is a reasonable to suggest that the interannual variation of river sediment is satisfied by the proposed SSD.

The following analysis considers the interannual sediment transport of the Yellow River Basin (Fig. 15), and all observed hydrological data (1955–1990) were obtained from the National Earth System Data Sharing Infrastructure, National Science & Technology Infrastructure of China (http://www.geodata.cn). Fortunately, we found that the SSD is also applicable to the interannual sediment transport series of rivers (Table 5, Fig. 16), showing dynamics similar to those of small watersheds. Generally, a debris

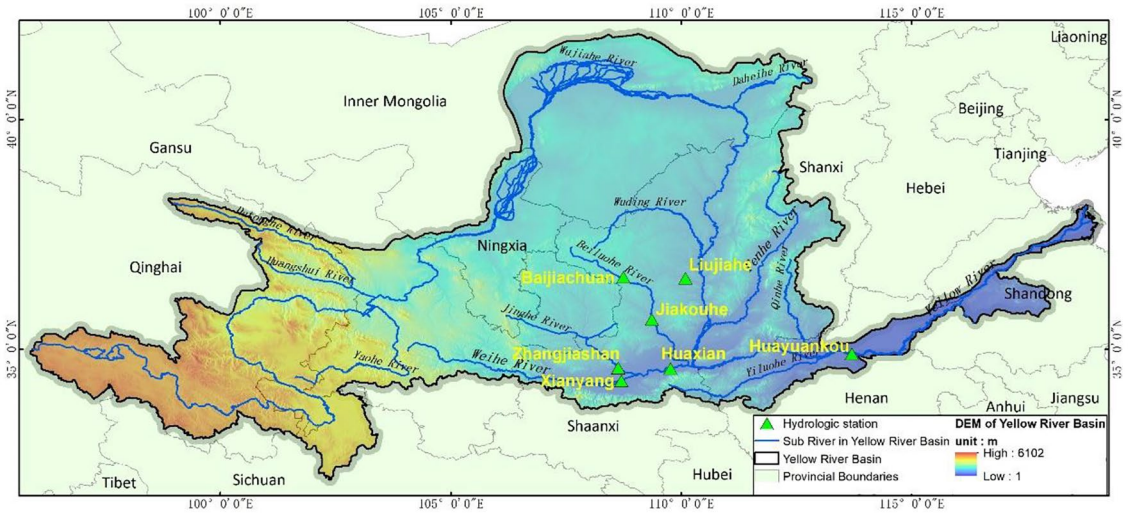

Fig. 15 Drainage map of the Yellow River Basin and location of hydrological stations

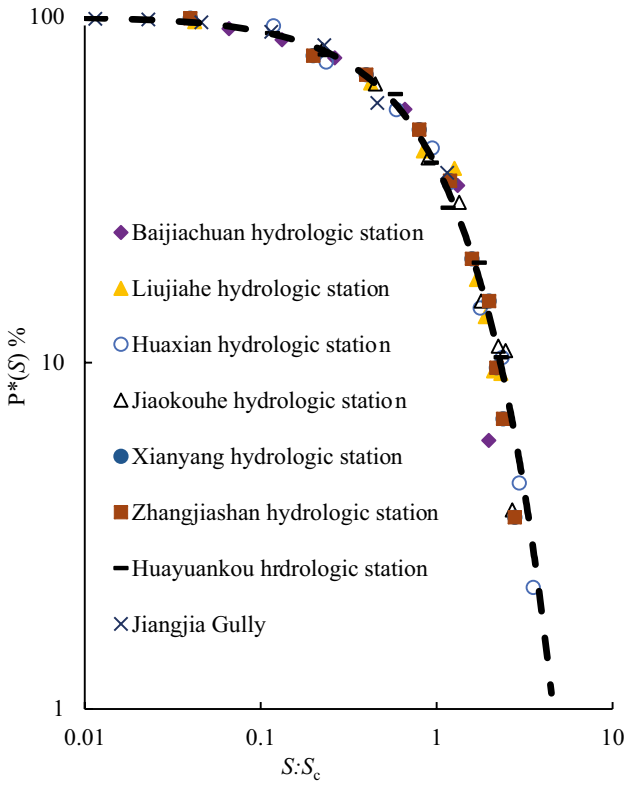

Fig. 16 Exponential distribution of sediment yield series of rivers

flow gully can be regarded as a branched source structure of a large river, with high soil activity and drastic sediment transport. For example, the values of CV and β of JJG are both bigger than those of rivers in the Yellow River Basin (Table 5), showing that the variability of sediment transport by debris flows is greater than that of rivers.

Spatially, different tributaries are at different stages of evolution, which causes obvious differences in the fluctuation and magnitude of the sediment transport process. Therefore, it is more realistic to discuss the change of parameter β in relation to different scales of the basin. It can be seen from Table 5 that the values of CV and β decrease gradually from the tributaries to the main channel, suggesting that the sediment transport process gradually becomes more stable. The value of parameter β of both the Jinghe River and the Beiluo River, which are secondary tributaries of the Yellow River, is approximately − 0.09. However, the value of parameter β of the Weihe River (a first tributary of the Yellow River) is approximately − 0.12, and that of the main channel is − 0.1972. This shows that parameter β not only reflects the spatial variation of sediment transport but also represents some dynamic process of basin evolution.

In practice, the SSD parameters change with the distribution of sediment yield; therefore, the total sediment yield (S_t) can be expressed by the SSD:

$$S_t = \int S_m p(S) dS \tag{11}$$

where S_m is the sediment yield at size S and $p(S)$ is the percentage. Considering that S_m varies with the ρ, v, and T of flows and is independent of size S, we have the following:

$$S_t = S_m \int p(S) dS = S_m(1 - P(S)) \tag{12}$$

where $P(S)$ is the SSD function defined by Eq. (7). Then, the change in sediment corresponds to the variation of β and S_c. This means that we can estimate the magnitude of the sediment in different basins using the SSD parameters.

Conclusions

This study investigated the spatiotemporal variation of sediment transport in terms of a debris flow surge series based on observational data. First, the fluctuation of sediment yield varies with the progress of the series and finally decays in a power law. It follows that some underlying system dynamics determine the process of sediment transport. Second, the cumulative sediment yield of the intermittent surges satisfies the unified sediment size distribution $P(S) = CS^{-\beta}\exp(-S/S_c)$, with parameters β and S_c describing the sediment transport features of the surges. A large value of β implies a greater percentage of "small" surges and a high decay property, and a large value of S_c indicates a wide range of fluctuation and high sediment transport capacity of debris flow events.

We determined the sediment size distribution of sediment transport and preliminarily discussed the physical meaning of parameters β and S_c. For all drainage basins, the diversity of soil sources and inhomogeneity of rainfall determine the random fluctuations of intermittent surges, but the unified distribution reveals the nonlinear dynamics of sediment transport. Further problems exist concerning the findings, among which the most urgent are to explore the universality of the SSD of sediments and to examine the variation of parameters in the process of sediment transport evolution based on observational data from drainage basins other than the Yellow River. The findings would be expected to provide further details regarding the dynamic characteristics of sediment transport series.

Acknowledgements

We are grateful for the data support from the "National Earth System Data Sharing Infrastructure, National Science & Technology Infrastructure of China (http://www.geodata.com)". We thank James Buxton MS_c, from Liwen Bianji (Edanz) (www.liwenbianji.cn/), for editing the English text of a draft of this manuscript.

Funding

This research is supported by the Sichuan Provincial Transportation Science and Technology Project (2021-A-08, 2021-A-04, 2021-A-03).

Data Availability

Data in this manuscript is public on "nsl.imde.ac.cn" and "http://www.geodata.cn" and will be made available on request.

Declarations

Competing interests The authors declare no competing interests.

References

Aronica GT, Candela A (2007) Derivation of flood frequency curves in poorly gauged Mediterranean catchments using a simple stochastic hydrological rainfall-runoff model. J Hydrol 347(1):132–142

Conaway CH, Draut AE, Echols KR, Storlazzi CD, Ritchie A (2013) Episodic suspended sediment transport and elevated polycyclic aromatic hydrocarbon concentrations in a small, mountainous river in coastal California. River Res Appl 29(7):919–932

Cui P (2000) The activity of debris flow and its contribution to river sediments in the downstream of Jingsha River: second academic seminar on mountain disasters and environmental conservation both sides of the Taiwan Straits, Taiwan-Taichung

Cui P, Chen XQ, Wang YY, Hu KH, Li Y (2005) Jiangjia Ravine debris flows in south-western China. Debris-flow hazards and related phenomena. Springer 565–594

Cui P, Wei FQ, Li Y (1999) Sediment transported by debris flow to the lower Jinsha River. Int J Sedim Res 14(4):67–71

Davies TRH (1986) Large debris flows: a macro-viscous phenomenon. Acta Mech 63(1–4):161–178

de Lima RE, Picanco JD, da Silva AF, Acordes FA (2020) An anthropogenic flow type gravitational mass movement: the Corrego do Feijao tailings dam disaster, Brumadinho. Brazil Landslides 17(12):2895–2906

Du RH, Kang ZC, Chen XQ, Zhu PY (1987) Investigation and prevention plan of debris flows in the Xiaojiang River, Yunnan. Science and Technology Literature Press, Chongqing, China

Eagleson PS (1972) Dynamics of flood frequency. Water Resour Res 8(4):878–898

Galewsky J, Stark CP, Dadson S, Wu CC, Sobel AH, Horng MJ (2006) Tropical cyclone triggering of sediment discharge in Taiwan. J Geophys Res Earth Surf 111(F3)

Glade T (2005) Linking debris-flow hazard assessments with geomorphology. Geomorphology 66(14):189–213

Govindaraju RS, Corradini C, Morbidelli R (2012) Local- and field-scale infiltration into vertically non-uniform soils with spatially-variable surface hydraulic conductivities. Hydrol Process 26(21):3293–3301

Grodek T, Jacoby Y, Morin E, Katz O (2012) Effectiveness of exceptional rainstorms on a small Mediterranean basin. Geomorphology 159:156–168

Guo XJ, Cui P, Su FH, Zhu XH, Wang CD (2013) Sediment transport characteristics in non-debris flow period in Jiangjia Gully. J Yangtze River Sci Res Inst 30(05):27–33 (in Chinese)

Guo XJ, Li Y, Cui P (2014) Experiment on random law of slope soil movement in the source area of debris flow. Journal of Jilin University. Earth Sci Ed 44(4):1260–1268

Hungr O, Evans SG (2001) A review of the classification of landslides of the flow type. Environ Eng Geosci 7(3):221–238

Imaizumi F, Tsuchiya S, Ohsaka O (2016) Field observations of debris-flow initiation processes on sediment deposits in a previous deep-seated landslide site. J Mt Sci 13(2):213–222

Iverson RM (1997) Hydraulic modeling of unsteady debris-flow surges with solid-fluid interactions. In: Proceedings of the 1997 1st International Conference on Debris-Flow Hazards Mitigation: Mechanics, Prediction, and Assessment, p 550–561

Jiang ZX (2015) Summary design of geological disaster Management in mountainous areas after Earthquake. Southwest Jiaotong University press. (in Chinese)

Lascelles B, Favis-Mortlock DT, Parsons AJ, Guerra AJT (2015) Spatial and temporal variation in two rainfall simulators: implications for spatially explicit rainfall simulation experiments. Earth Surf Proc Land 25(7):709–721

Li Y, Chen XQ, Hu KH, He SF (2005) Fractality of grain composition of debris flows. J Geog Sci 15(3):353–359

Li Y, Huang CM, Wang BL, Tian XF, Liu JJ (2017) A unified expression for grain size distribution of soils. Geoderma 288:105–119

Li Y, Liu J, Chen XQ, Wei FQ (2007) Grain composition and erosive equilibrium of debris flows. J Mt Sci 4(1):071–076

Li Y, Liu JJ, Su FH, Xie J, Wang BL (2015) Relationship between grain composition and debris flow characterstics, a case study of the jiangjia Gully in China. Landslides 12:19–28

Li Y, Su PC, Su FH (2011) Debris flow as a spatial Poisson process. J Mt Sci 29(5):586–590

Li Y, Zhou XJ, Su PC, Kong YD, Liu JJ (2013) A scaling distribution for grain composition of debris flow. Geomorphology 192:30–42

Lin CW, Shieh CL, Yuan BD, Shieh YC, Liu SH, Lee SY (2004) Impact of Chi-Chi earthquake on the occurrence of landslides and debris flows: example from the Chenyulan River watershed, Nantou. Taiwan Eng Geol 71(1–2):49–61

Liu JJ, Li Y, Su PC, Cheng ZL, Cui P (2009) Temporal variation of intermittent surges of debris flow. J Hydrol 365(3):322–328

Major JJ (1997) Depositional processes in large-scale debris-flow experiments. J Geol 105(3):345–366

Milliman DJ, Farnsworth LK (2011) River discharge to the Coastal Ocean: a global synthesis, Cambridge. Cambridge Univ, Press

Prancevic JP, Michael PL, Brian MF (2014) Incipient sediment motion across the river to debris-flow transition. Geology 42(3):191–194

Read LK, Vogel RM (2016) Hazard function analysis for flood planning under nonstationarity. Water Resour Res 52(5):4116–4131

Rickenmann D, Badoux A, Hunzinger L (2016) Significance of sediment transport processes during piedmont floods: the 2005 flood events in Switzerland. Earth Surf Proc Land 41(2):224–230

Rickenmann D, Koschni A (2010) Sediment loads due to fluvial transport and debris flows during the 2005 flood events in Switzerland. Hydrol Process 24(8):993–1007

Royall D, Kennedy L (2016) Historical erosion and sedimentation in two small watersheds of the southern Blue Ridge Mountains, North Carolina, USA. Catena 143:174–186

Sadeghi S, Mizuyama T, Miyata S, Gomi T, Kosugi K, Fukushima T, Mizugaki S, Onda Y (2008) Development, evaluation and interpretation of sediment rating curves for a Japanese small mountainous reforested watershed. Geoderma 144(1):198–211

Sepúlveda SA, Moreiras SM, Lara M, Alfaro A (2015) Debris flows in the Andean ranges of central Chile and Argentina triggered by 2013 summer storms: characteristics and consequences. Landslides 12(1):115–133

Slaymaker O (1993) The sediment budget of the Lillooet River basin, British Columbia. Phys Geogr 14(3):304–320

Syvitski JPM, James PM, John DM (2007) Geology, geography, and humans battle for dominance over the delivery of fluvial sediment to the coastal ocean. J Geol 115(1):1–19

Takahashi T (2014) Debris flow: mechanics, prediction and countermeasures. CRC Press

Takayama S, Satofuka Y, Imaizumi F (2022) Effects of water infiltration into an unsaturated streambed on debris flow development. Social Science Electronic Publishing Geomorphology 409:108269

Tang C, Zhu J, Ding J, Cui XF, Chen L, Zhang JS (2011) Catastrophic debris flows triggered by a 14 August 2010 rainfall at the epicenter of the Wenchuan earthquake. Landslides 8(4):485–497

Warrick JA, Melack JM, Goodridge BM (2015) Sediment yields from small, steep coastal watersheds of California. J Hydrol Reg Stud 4:516–534

Warrick JA, Mertes LAK (2009) Sediment yield from the tectonically active semiarid Western Transverse Ranges of California. Geol Soc Am Bull 121(7–8):1054–1070

Wilford DJ, Sakals ME, Innes JL, Bergerud WA (2004) Recognition of debris flow, debris flood and flood hazard through watershed morphometrics. Landslides 1(1):61–66

Wu JS, Kang ZC, Lian TQ, Zhang SC (1990) Observation and research on the debris flows in Jiangjia Gully, Yunnan Province. Science Press, Beijing, China (in Chinese)

Yue S, Ouarda T, Bobée B, Legendre P, Bruneau P (1999) The Gumbel mixed model for flood frequency analysis. J Hydrol 226(1):88–100

Daochuan Liu · Yang Jia · Yunyong He (✉) · Jiang Shao · Bo Xiang · Miao Liang
Sichuan Highway Planning, Survey, Design and Research Institute Ltd, Chengdu 610041, China
Email: heyuny2022@163.com

Daochuan Liu
Key Laboratory of Mountain Hazards and Earth Surface Processes, and Institute of Mountain Hazards and Environment, Chinese Academy of Sciences, Chengdu 610041, China

Yunyong He
Southwest Jiaotong University, Chengdu 610041, China
Email: heyuny2022@163.com

Daochuan Liu Jiang Shao Miao Liang
Sichuan Tongchuan Engineering Technology Development Co., Ltd, Chengdu 610041, China

Fuming Wang Chengchao Guo
School of Civil Engineering, Sun Yat-sen University, Guangzhou 510275, China

Fuming Wang Chengchao Guo
Southwest Jiaotong University, Chengdu 610032, China